This article can be cited as A. Widyotriatmo and K.-S. Hong, Configuration Control of an Autonomous Vehicle under Nonholonomic and Field-of-View Constraints, International Journal of Imaging and Robotics, vol. 15, no. 3, pp. 126-139, 2015.

Configuration Control of an Autonomous Vehicle under Nonholonomic and Field-of-View Constraints

Augie Widyotriatmo[1] and Keum-Shik Hong[2]

[1]Instrumentation and Control Research Group, Faculty of Industrial Technology
Bandung Institute of Technology,Ganesha 10, 40132 Bandung (Indonesia);
Email: augie@tf.itb.ac.id

[2]Department of Cogno-Mechatronics Engineering and School of Mechanical Engineering
Pusan National University, 30 Jangjeon-dong, Geumjeong-gu, 609-735 Busan (Korea);
Email: kshong@pusan.ac.kr

ABSTRACT

In this paper, a configuration (position and orientation) control problem of a forklift under the field-of-view (FOV) constraint of a camera is considered. In designing a control law, three navigation variables (the distance error, two split angles of the orientation error) are utilized. The control problem is formulated as an asymptotic stabilization problem of the origin in the error space of the navigation variables, in which the orientation error associated with the direction of the vehicle to the goal point is constrained within the camera's FOV. A barrier function (a continuous function whose value increases to infinity when its argument approaches the boundary of a constrained region) is used as a Lyapunov function candidate. The designed control law ensures the asymptotic stability of the origin, whereas the given constraint is never violated. The performance of the proposed method is compared with that without the FOV constraint. The effectiveness of the proposed method is demonstrated by experimental results of pallet picking.

Keywords: Configuration control, autonomous vehicle, forklift, nonholonomic constraint, visual servo, field-of-view constraint.

Mathematics Subject Classification: 93C85, 93D15

Computing Classification System: I.2.9, I.4

1. INTRODUCTION

Mobile robots have been used in many applications including material handling vehicles, security patrols, environment surveillance, and many more. This paper presents the development of an autonomous forklift for the material handling industry. The following specific technologies have been developed: In (Tamba, Hong, & Hong, 2009), path following of the generated path; In (Widyotriatmo, Hong, & Hong 2009; Widyotriatmo, Hong, & Prayudhi, 2010; Widyotriatmo & Hong, 2012), configuration control to load/unload a pallet at a fixed locationl reactive obstacle avoidance to evade collisions with unmodeled obstacles and other vehicles in the environment; In (Widyotriatmo & Hong, 2011) the generation of a collision-free path from an initial position to a goal point; Widyotriatmo & Hong (2013) propose a control architecture that integrates the control algorithms so that an autonomous forklift performs proper action. In this paper, the pallet picking operation of a forklift using a camera, which measures the pallet's configuration, is the focus. The control objective is to move the

forklift from an initial to a pallet configuration while the pallet's feature remains visible through the camera from the beginning to the end.

Vision systems have been proven successful in identifying and extracting an object's configurations (Gusrialdi et al., 2013; Pásztó et al. 2014). The use of such systems for mobile robot control has been addressed in a number of studies. In (Zhang & Ostrowski, 2002), a mobile robot trajectory planning based upon the image features extracted from visual data was proposed. Seelinger and Yoder (2006) present a pallet engagement strategy integrating a vision system with an autonomous forklift. The shortest path of a mobile robot subject to nonholonomic constraints and a limited FOV was studied in (Salaris, Fontanelli, & Pallatino, 2010). Optimal path planning methods that maintained the visibility of a fixed landmark for mobile robots were explored in (Bhattacharya, Murrieta-Cid, Hutchinson, 2007). In (Van Den Berg, Abbeel, & Goldberg, 2011), an optimized path planning method for robots considering FOV of camera method was proposed. In those previous literature, the paths/trajectories were calculated offline, and control algorithms were designed to keep the vehicles on those paths/trajectories. In (Lopez-Nicolas & Sagues, 2011), a vision-based exponential stabilization of mobile robots was proposed, but any FOV constraint was not taken into account. Sequential control laws to drive a mobile robot from an initial to a goal configuration while maintaining the visibility of a landmark were proposed in (Kantor & Rizzi, 2005; Mariottini, Oriolo, & Prattichizzo, 2007; Amarasinghe, Mann, & Gosine, 2007; Lopes & Koditschek, 2007; Beccera, Lopez-Nicolas, & Sagues, 2011).

This paper proposes a control law that drives a forklift from an initial to a goal configuration while maintaining the feature specifying the goal configuration within the view of the camera. In designing the control law, three navigation variables (i.e., the distance error and two split angles of the orientation error, one in association with the direction to the goal point and the other in association with the desired direction at the goal point) are utilized. The FOV constraint of the camera is included in the control design by limiting the orientation error associated with the direction to the goal point within a certain value range. To deal with the FOV constraint, a barrier function is utilized as a Lyapunov function candidate. In (Tee, Ge, & Tay, 2009), a barrier function method was proposed for single-input-single-output (SISO) nonlinear systems with output constraint. In (Ngo, Mahony, & Jiang, 2005; Tee & Ge, 2009), barrier function methods dealt with nonlinear systems with state constraints, in which offline optimization methods for determining control parameters to maintain states inside the constraint range are utilized. The novelty of this paper is the proposed barrier function method in designing the configuration control for a wheeled vehicle with a limited FOV constraint, which is classified as a multi-input-multi-output (MIMO) nonlinear system with a state constraint. The designed control law assures the negative semi-definiteness of the time derivative of the Lyapunov function and the boundedness of the barrier function. Using the LaSalle's theorem and a lemma for the use of barrier function as a Lyapunov function candidate, the asymptotic stability of the origin of navigation variables is guaranteed while the constraint is never violated.

The main contribution of the paper is the design of a smooth control law that assures the asymptotic stability of the origin of navigation variables while the FOV constraint is never violated. The control

This article can be cited as A. Widyotriatmo and K.-S. Hong, Configuration Control of an Autonomous Vehicle under Nonholonomic and Field-of-View Constraints, International Journal of Imaging and Robotics, vol. 15, no. 3, pp. 126-139, 2015.

gains, designed without using offline optimization methods, determine a desired performance of the closed-loop systems in a neighborhood of the origin, and a fast convergence of the states to the origin is achieved. Comparisons between the motion of the forklift using the proposed method and that using the control laws with no FOV constraint are presented. Experimental results of a pallet picking of an autonomous forklift are demonstrated.

The paper is organized as follows. Section 2 formulates the problem, being the kinematic model of a typical forklift and the FOV constraint. Section 3 introduces the barrier function, derives the control law, and elucidates the design of control gains. Section 4 presents simulation and experimental results on the autonomous forklift. Section 5 draws conclusions.

2. PROBLEM DESCRIPTION

Figure 1 shows a schematic of the forklift having two caster wheels in the front and one drivable-and-steerable wheel in the rear. O-$\hat{i}\hat{j}$ represents the global reference coordinate frame in the workspace, O_b-$\hat{i}_\mathrm{b}\hat{j}_\mathrm{b}$ denotes the body coordinate frame attached to the vehicle body where O_b (the mid-point of two front wheels) is the origin of the frame to which all the motions of the vehicle are generated, and l denotes the distance between the center of the rear wheel and O_b. The vehicle's configuration is specified by its position (x, y) and orientation θ, which is the orientation angle of the $\hat{i}_\mathrm{b}$-axis from the $\hat{i}$-axis (in the counterclockwise direction). The control inputs of the considered forklift are the driving velocity v and the steering angle δ in $[-\pi/2, \pi/2]$, both of which are applied at the rear wheel. The kinematic equations of the forklift are:

$$\dot{x} = v\cos\theta\cos\delta, \tag{1}$$

$$\dot{y} = v\sin\theta\cos\delta, \tag{2}$$

$$\dot{\theta} = -(v/l)\sin\delta. \tag{3}$$

Let O_g-$\hat{i}_\mathrm{g}\hat{j}_\mathrm{g}$ be the goal coordinate frame, where (x_g, y_g) be the coordinates of the goal point O_g and θ_g is the rotational angle of the $\hat{i}_\mathrm{g}$-axis from $\hat{i}$-axis. Let $\tilde{x} = x_\mathrm{g} - x$, $\tilde{y} = y_\mathrm{g} - y$, and $\tilde{\theta} = \theta_\mathrm{g} - \theta$ be the configuration error between the current and goal configurations. Let three new variables {ρ, α, ϕ} (i.e., navigation variables) be defined as follows: $\rho = \sqrt{\tilde{x}^2 + \tilde{y}^2}$ is the distance error, $\alpha = \arctan 2(\tilde{y}, \tilde{x}) - \theta$ and $\phi = \theta_\mathrm{g} - \arctan 2(\tilde{y}, \tilde{x})$ are the split portions of the orientation error (i.e., $\tilde{\theta}$ = α + ϕ), in which α is the portion from the vehicle's moving direction to the goal point direction and ϕ is the remaining portion at the goal frame. The kinematic equations of the forklift using the introduced navigation variables are obtained as follows.

This article can be cited as A. Widyotriatmo and K.-S. Hong, Configuration Control of an Autonomous Vehicle under Nonholonomic and Field-of-View Constraints, International Journal of Imaging and Robotics, vol. 15, no. 3, pp. 126-139, 2015.

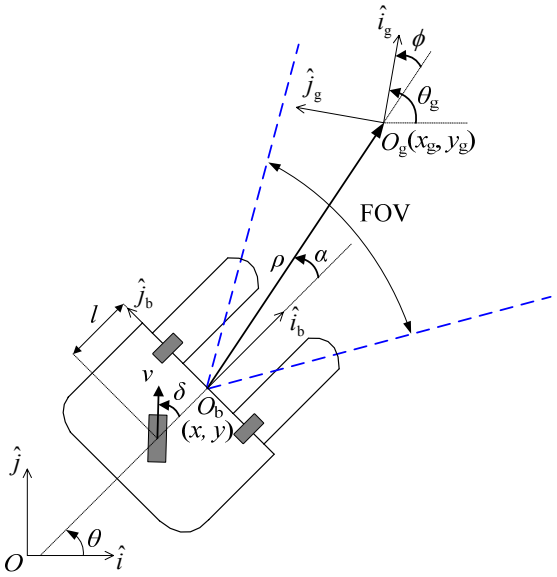

Figure. 1. Forklift schematic: **The** two dashed-lines represent the boundaries of the view that can be imaged by the camera.

$$\dot{\rho} = -v\cos\alpha\cos\delta\,, \tag{4}$$

$$\dot{\alpha} = (v/\rho)\sin\alpha\cos\delta + (v/l)\sin\delta\,, \tag{5}$$

$$\dot{\phi} = -(v/\rho)\sin\alpha\cos\delta\,. \tag{6}$$

The kinematic equations (4)-(6) are valid for non-zero distance ρ, since both α and ϕ are not defined if ρ = 0. In this paper, it is assumed that the initial distance error is nonzero, that is, $\rho(0) \geq \rho_\varepsilon > 0$, where ρ_ε is a small positive constant. If the vehicle achieves its goal configuration, all ρ, α, and ϕ become zero. Then, the control problem of moving a vehicle from one configuration to another becomes an asymptotic stabilization problem of the system (4)-(6) to the origin.

A camera, affixed at the reference point O_b, is utilized to identify the target feature and to measure the target configuration. The principal axis of the camera always coincides with the $\hat{i}_b$-axis. In Figure 1, the horizontal FOV of the camera is the angle between the two dashed lines. In this paper, we only consider the horizontal FOV, and therefore there are no restrictions on the vertical FOV. Let the FOV of the camera be FOV = $2\bar{\alpha} < \pi$. In order that the goal point always stays inside the boundaries of the view of the camera, the orientation error associated with the direction to the goal point (α) is constrained by

$$|\alpha| < \bar{\alpha} < \pi/2\,. \tag{7}$$

This article can be cited as A. Widyotriatmo and K.-S. Hong, Configuration Control of an Autonomous Vehicle under Nonholonomic and Field-of-View Constraints, International Journal of Imaging and Robotics, vol. 15, no. 3, pp. 126-139, 2015.

3. CONTROL DESIGN

In this section, a control law that asymptotically stabilizes the origin of (4)-(6) without violating the constraint (7) is derived. The vehicle model considered is ideal, with no uncertainties. A barrier function $V_b(z):(-\bar{z},\bar{z})\to R^+$, which is a continuous function on $(-\bar{z},\bar{z})$, is positive definite, and goes to infinity as $z\to\pm\bar{z}$, is utilized. An example of barrier functions (Ngo et al., 2005; Tee et al., 2009) is

$$V_b(z)=(1/2)\ln\left(\bar{z}^2/\left(\bar{z}^2-z^2\right)\right). \tag{8}$$

The following lemma shows the use of a barrier function as a Lyapunov function candidate for a control design.

Lemma: Let $z(t)=[z_1(t),\ldots,\ z_{n_z}(t)]^T\in R^{n_z}$. Let $\Omega_z=\{z(t)\in R^{n_z}:\left|z_i(t)\right|<\bar{z}_i,\ i=1,\ldots,\ n_z\}$. Consider the system

$$\dot{z}(t)=f(t,z), \tag{9}$$

where f: $R^+\times R^{n_z}\to R^{n_z}$. Let $V_i:\left(-\bar{z}_i,\bar{z}_i\right)\to R+$, $i=1,\ \ldots,\ n_z$, be positive definite functions that are continuously differentiable on Ω_z. Let $V_i(z_i)\to\infty$ as $z_i\to\pm\bar{z}_i$, i = 1, …, n_z. Let $V(z(t))=\sum_{i=1}^{n_z}V_i(z_i(t))$ and $z(0)\in\Omega_z$. If

$$\dot{V}(z(t))\le 0, \tag{10}$$

in the set Ω_z, it follows that $z(t)\in\Omega_z$ for $t\in[0,\infty)$.

Proof: Since V is a positive definite function, the negative semidefinite form in (5) implies that $V(z(t))\le V(z(0))\quad\forall t\in[0,\infty)$, that is, $V(z(t))$ is bounded $\forall t\in[0,\infty)$. Since $V(z)=\sum_{i=1}^{n_z}V_i(z_i)$ is a positive definite function, then $\sum_{i=1}^{n_z}V_i(z_i)$ becomes bounded $\forall t\in[0,\infty)$. From the property of the barrier function, that is, $V_i(z_i)\to\infty$ only if $z_i\to\pm\bar{z}_i$, $i=1,\ \ldots,\ n_z$, and given that $z_i(0)\in\Omega_z$, it can be concluded that $z_i(t)\in\Omega_z$, $i=1,\ \ldots,\ n_z$, $\forall t\in[0,\infty)$. □

Let $v_1=v\cos\delta$ and $v_2=v\sin\delta$. The linear velocity and steering angle in terms of v_1 and v_2 are $v=\mathrm{sgn}(v_1)\sqrt{v_1^2+v_2^2}$ and $\delta=\arctan(v_2/v_1)$. Let v_1 and v_2 be designed as

$$v_1=k_{v,1}\rho\cos\alpha, \tag{11}$$

$$v_2=-l\left(k_{v,2}\sin\alpha\cos\alpha-k_{v,3}\phi\left(\sin^2\bar{\alpha}-\sin^2\alpha\right)\right), \tag{12}$$

where $k_{v,1}$, $k_{v,2}$, and $k_{v,3}$ are positive constants. Then, equations (4)-(6) become

$$\dot{\rho}=-k_{v,1}\rho\cos^2\alpha, \tag{13}$$

This article can be cited as A. Widyotriatmo and K.-S. Hong, Configuration Control of an Autonomous Vehicle under Nonholonomic and Field-of-View Constraints, International Journal of Imaging and Robotics, vol. 15, no. 3, pp. 126-139, 2015.

$$\dot{\alpha} = -\left(k_{v,2} - k_{v,1}\right)\sin\alpha\cos\alpha + k_{v,1}k_{v,3}\phi(\sin^2\bar{\alpha} - \sin^2\alpha), \tag{14}$$

$$\dot{\phi} = -k_{v,1}\sin\alpha\cos\alpha. \tag{15}$$

Let a Lyapunov function be chosen as

$$\begin{aligned} V &= V_1 + V_2 + V_3 \\ &= \frac{1}{2}\rho^2 + \frac{1}{2}\ln\left(\frac{\sin^2\bar{\alpha}}{\sin^2\bar{\alpha} - \sin^2\alpha}\right) + \frac{1}{2}k_{v,3}\phi^2. \end{aligned} \tag{16}$$

By setting $k_{v,2} > k_{v,1}$, the time derivative of V becomes

$$\dot{V} = -k_{v,1}\rho^2\cos^2\alpha - \frac{\left|k_{v,2} - k_{v,1}\right|\sin^2\alpha\cos^2\alpha}{\sin^2\bar{\alpha} - \sin^2\alpha}. \tag{17}$$

Then, $\dot{V} \le 0$ in the set $|\alpha| \le \bar{\alpha}$.

Theorem: Consider the system (4)-(6). Let the control law be chosen as

$$v = \left(\left(k_{v,1}\rho\cos\alpha\right)^2 + l^2\left(k_{v,2}\sin\alpha\cos\alpha - k_{v,3}\phi\left(\sin^2\bar{\alpha} - \sin^2\alpha\right)\right)^2\right)^{1/2}, \tag{18}$$

$$\delta = -\arctan\left(l\frac{k_{v,2}\sin\alpha\cos\alpha - k_{v,3}\phi\left(\sin^2\bar{\alpha} - \sin^2\alpha\right)}{k_{v,1}\rho\cos\alpha}\right). \tag{19}$$

If the initial condition satisfies $|\alpha(0)| < \bar{\alpha} < \pi/2$, α never violates its constraint, that is, $|\alpha(t)| < \bar{\alpha}$ for $t \in [0, \infty)$. Furthermore, the origin (ρ, α, ϕ) = (0, 0, 0) is uniformly asymptotically stable.

Proof: First, we show that $|\alpha(t)| < \bar{\alpha}$ for $t \in [0, \infty)$. From (17), $\dot{V}$ is negative semidefinite in the set $|\alpha| < \bar{\alpha}$. Since V_1, V_2, and V_3 are positive definite functions, $V_2(t)$ is always bounded for $t \in [0, \infty)$. Referring to the lemma, if $|\sin\alpha(0)| < \sin\bar{\alpha}$, it follows that $|\sin\alpha(t)| < \sin\bar{\alpha}$ for $t \in [0, \infty)$. Since $|\alpha(0)| < \bar{\alpha} < \pi/2$, it can be obtained that $|\alpha(t)| < \bar{\alpha}$ for $t \in [0, \infty)$.

Now, we show that the origin (ρ, α, ϕ) = (0, 0, 0) is asymptotically stable. Let the set $S = \{(\rho, \alpha, \phi) : \dot{V} = 0\}$. From (17), It can be seen that $\rho(t)$, $\alpha(t)$ go to zero as time goes to infinity or $S = \{(\rho, \alpha, \phi) : \rho = \alpha = 0\}$. Let $\rho(t)$, $\alpha(t)$, and $\phi(t)$ be the solutions identically to S, $\alpha(t) = 0$ implies that $\dot{\alpha}(t) = 0$. Then, from (14), it will be obtained $\phi(t) = 0$. The only solutions that can stay identically in S are $\rho(t) = \alpha(t) = \phi(t) = 0$. Thus it is obtained that $\rho, \alpha, \phi \to 0$ as $t \to \infty$. □

This article can be cited as A. Widyotriatmo and K.-S. Hong, Configuration Control of an Autonomous Vehicle under Nonholonomic and Field-of-View Constraints, International Journal of Imaging and Robotics, vol. 15, no. 3, pp. 126-139, 2015.

Remark 1: The linearization of (13)-(15) at the origin yields

$$\begin{bmatrix}\dot{\rho}\\ \dot{\alpha}\\ \dot{\phi}\end{bmatrix}=\begin{bmatrix}-k_{v,1} & 0 & 0\\ 0 & -(k_{v,2}-k_{v,1}) & k_{v,1}k_{v,3}\sin^2\overline{\alpha}\\ 0 & -k_{v,1} & 0\end{bmatrix}\begin{bmatrix}\rho\\ \alpha\\ \phi\end{bmatrix}. \tag{20}$$

The spectrum of the matrix in (22) can be completely assigned by $k_{v,1}$, $k_{v,2}$, and $k_{v,3}$. In our method, $k_{v,1}$, $k_{v,2}$, and $k_{v,3}$ are designed as $k_{v,2} > k_{v,1} > 0$ and $k_{v,3} = \left(k_{v,2}-k_{v,1}\right)^2 / \left(4k_{v,1}^2\sin^2\overline{\alpha}\right)$. Then, one eigenvalue of the matrix in (22) becomes $-k_{v,1}$ and the other two are $-\left|k_{v,2}-k_{v,1}\right|/2$.

Remark 2: The control law (20)-(21) do not guarantee the convergence of the steering angle δ to zero. However, the asymptotic stability of the origin (ρ, α, ϕ) = (0, 0, 0) is assured.

Remark 3: In the presence of model uncertainty and measurement noise, the convergence of the solutions of (4)-(6) to zero may not be achieved. However, refering to the asymptotical stability in the ideal case, the control law ensures uniformly bounded solutions.

4. SIMULATION AND EXPERIMENTAL RESULTS

4.1. Simulation

In this section, the performance of the proposed control law is verified by simulation. The simulation is done by solving equations (1)-(3) with the control laws (18)-(19) as in Huusom et al. (2010), . Precup et al. (2011), Joelianto et al. (2013), and Jafarnejadsani et al. (2013).

For comparison, the control laws without considering the FOV constraint in (Widyotriatmo & Hong, 2012) and (Siegwart & Nourbakhsh, 2004) are simulated. The control law proposed in (Widyotriatmo & Hong, 2012) is

$$v=\left(\left(k_{v,1}\rho\right)^2+l^2\left(k_{v,2}\alpha-k_{v,3}\phi\right)^2\right)^{1/2}, \tag{21}$$

$$\delta=-\arctan\left(l\left(k_{v,2}\alpha-k_{v,3}\phi\right)/\left(k_{v,1}\rho\right)\right), \tag{22}$$

where $k_{v,1}$, $k_{v,3}$ > 0 and $k_{v,2} > (2/\pi)k_{v,1} + (5/3)k_{v,3}$.

The control law proposed in (Siegwart & Nourbakhsh, 2004) is

$$v=\left(\left(k_{v,1}\rho\cos\alpha\right)^2+l^2\left(k_{v,2}\alpha+k_{v,1}(\alpha-k_{v,3}\phi)\cos\alpha\sin\alpha/\alpha\right)^2\right)^{1/2}, \tag{23}$$

$$\delta=-\arctan\left(l\frac{k_{v,2}\alpha+k_{v,1}(\alpha-k_{v,3}\phi)\cos\alpha\sin\alpha/\alpha}{k_{v,1}\rho\cos\alpha}\right), \tag{24}$$

where $k_{v,1}$, $k_{v,2} > 0$ and $k_{v,3} = k_{v,2}^2/4k_{v,1}^2$.

To compare the performance of the control laws with and without the FOV constraint, a navigation from the initial configuration (x, y, θ) = (−1, −1.5, 1) to the goal configuration (x, y, θ) = (0, 0, 0) is

This article can be cited as A. Widyotriatmo and K.-S. Hong, Configuration Control of an Autonomous Vehicle under Nonholonomic and Field-of-View Constraints, International Journal of Imaging and Robotics, vol. 15, no. 3, pp. 126-139, 2015.

simulated. The unit of x and y is in meter and that of θ is rad. The FOV of the camera is 0.28π rad, and therefore the constraint becomes $|\alpha| < 0.14\pi$ rad. In using (18)-(19), the control gains are set to $k_{v,1} = 0.5\ \text{s}^{-1}$, $k_{v,2} = 2\ \text{s}^{-1}$, and $k_{v,3} = 12.4\ \text{s}^{-1}$. Using (21)-(22), $k_{v,1} = 0.5\ \text{s}^{-1}$, $k_{v,2} = 4\ \text{s}^{-1}$, and $k_{v,3} = 2\ \text{s}^{-1}$. Using (23)-(24), $k_{v,1} = 0.5\ \text{s}^{-1}$, $k_{v,2} = 2\ \text{s}^{-1}$, and $k_{v,3} = 4\ \text{s}^{-1}$.

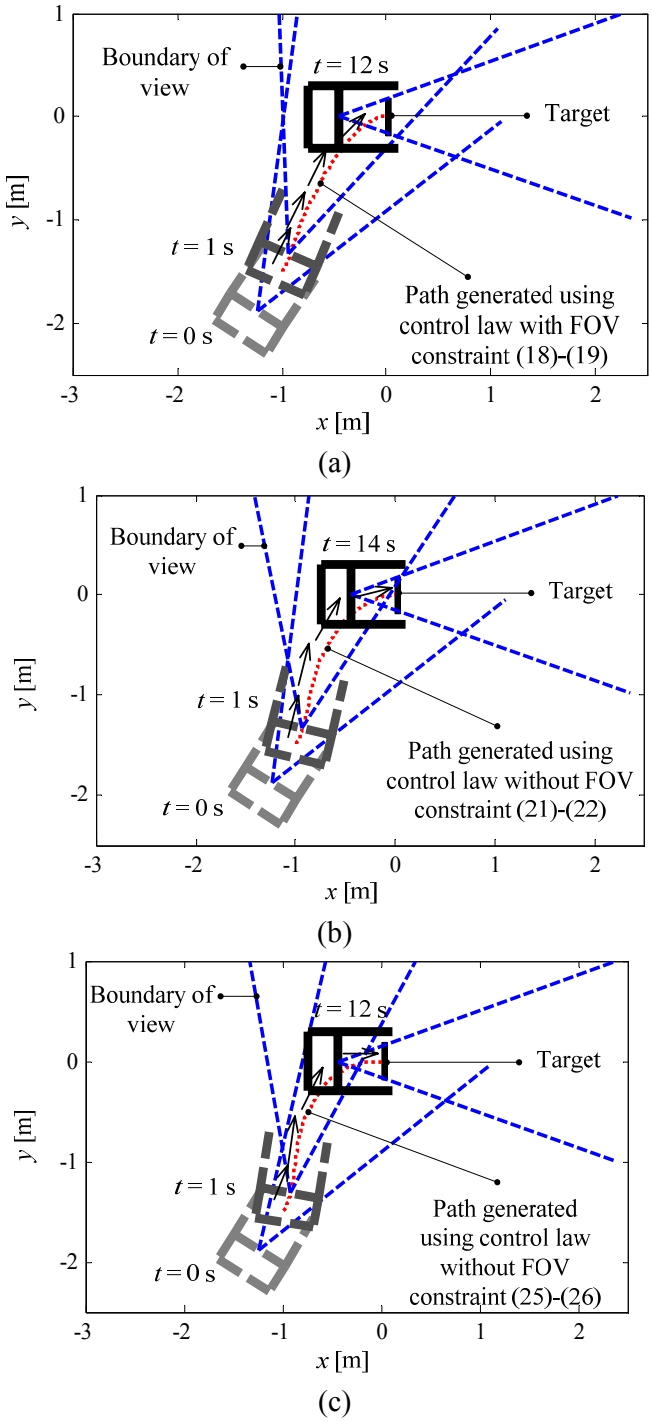

Figure. 2. Comparison of configuration control laws with and without the consideration of FOV constraint: (a) using (18)-(19), (b) using (21)-(22), (c) using (23)-(24).

This article can be cited as A. Widyotriatmo and K.-S. Hong, Configuration Control of an Autonomous Vehicle under Nonholonomic and Field-of-View Constraints, International Journal of Imaging and Robotics, vol. 15, no. 3, pp. 126-139, 2015.

The trajectories of the forklift to the target configuration under three different control laws, (18)-(19), (21)-(22), and (23)-(24), are compared in Figures 2(a), 2(b), and 2(c), respectively. Using (18)-(19), the forklift keeps the target feature inside the FOV, whereas, using (21)-(22) and (23)-(24), the target feature goes out the FOV at $t = 1$ s. The configuration motions, α, v, and δ are depicted in Figures 3-6, respectively. In Figure 3, the trajectories of x, y, and θ tend to zero using the three control laws (18)-(19), (21)-(22), and (23)-(24). In Figure 4, using (18)-(19), α never violates its constraint. However, using (21)-(22) and (23)-(24), α violates its constraint from 0.4 s to 1.6 s and from 0.3 s to 2.5 s, respectively. In both time spans, the target feature is lost from the camera view.

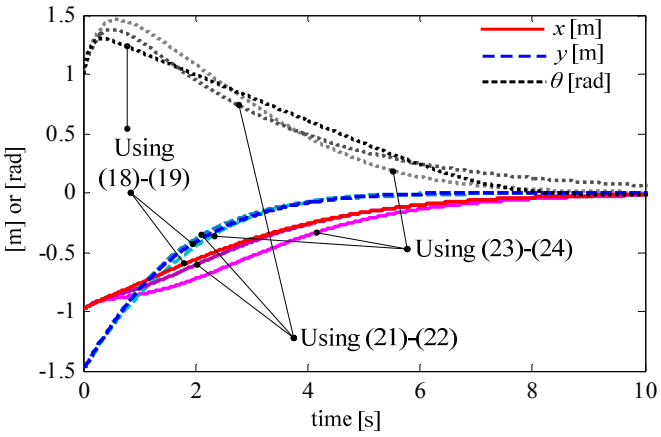

Figure 3. Configuration motions using (18)-(19), (21)-(22), and (23)-(24). All trajectories of x, y, and θ tend to zero.

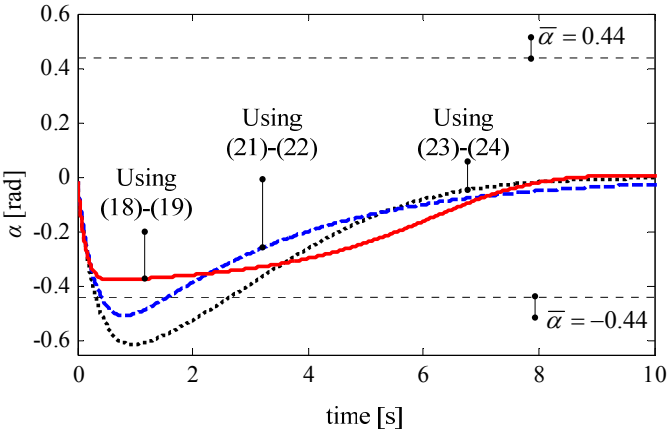

Figure 4. α using (18)-(19), (21)-(22), and (23)-(24). Using (18)-(19), α never violate the constraint $\bar{\alpha}$ while both (21)-(22) and (23)-(24) α violates its constraint from 0.4 s to 1.6 s and from 0.3 s to 2.5 s, respectively.

This article can be cited as A. Widyotriatmo and K.-S. Hong, Configuration Control of an Autonomous Vehicle under Nonholonomic and Field-of-View Constraints, International Journal of Imaging and Robotics, vol. 15, no. 3, pp. 126-139, 2015.

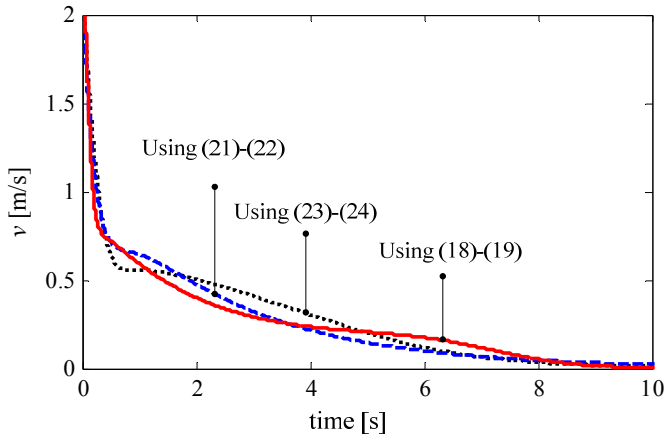

Figure 5. v using (18)-(19), (21)-(22), and (23)-(24).

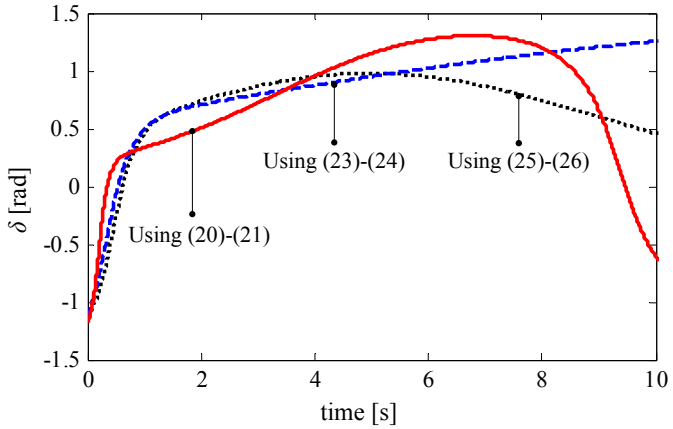

Figure 6. δ in Figure 2: using (18)-(19), (21)-(22), and (23)-(24).

4.2. Experiment

In this section, the effectiveness of the proposed method is evaluated by experiment. The control law (18)-(19) is implemented to the forklift engaging a pallet detected by a camera. Figure 7(a) shows the forklift employed in the experiment. The forklift is equipped with a PC, a programmable logic controller (PLC), a laser-based localization sensor SICK NAV200 for determination of the vehicle configuration in the global coordinate, a camera (FOV 0.28π rad) for measuring the configuration of a pallet, and a laser range finder (LRF) for detecting obstacles. The forklift implements a two-loop (outer and inner) control strategy. The outer loop, programmed in C++ on the PC, computes the control commands (linear velocity and steering angle) of the driving wheel, and the inner loop, programmed in PLC, computes the voltages supplied to two AC motors (driving and steering) using a proportional-derivative (PD) algorithm in the fashion that the linear velocity and steering angle of the driving wheel follow their desired commands. The chessboard pattern and the corners detected by the vision system are shown in Figure 7(b).The control gains are set to $k_{v,1} = 0.3\ \mathrm{s}^{-1}$, $k_{v,2} = 1\ \mathrm{s}^{-1}$, and $k_{v,3} = 7.5\ \mathrm{s}^{-1}$.

This article can be cited as A. Widyotriatmo and K.-S. Hong, Configuration Control of an Autonomous Vehicle under Nonholonomic and Field-of-View Constraints, International Journal of Imaging and Robotics, vol. 15, no. 3, pp. 126-139, 2015.

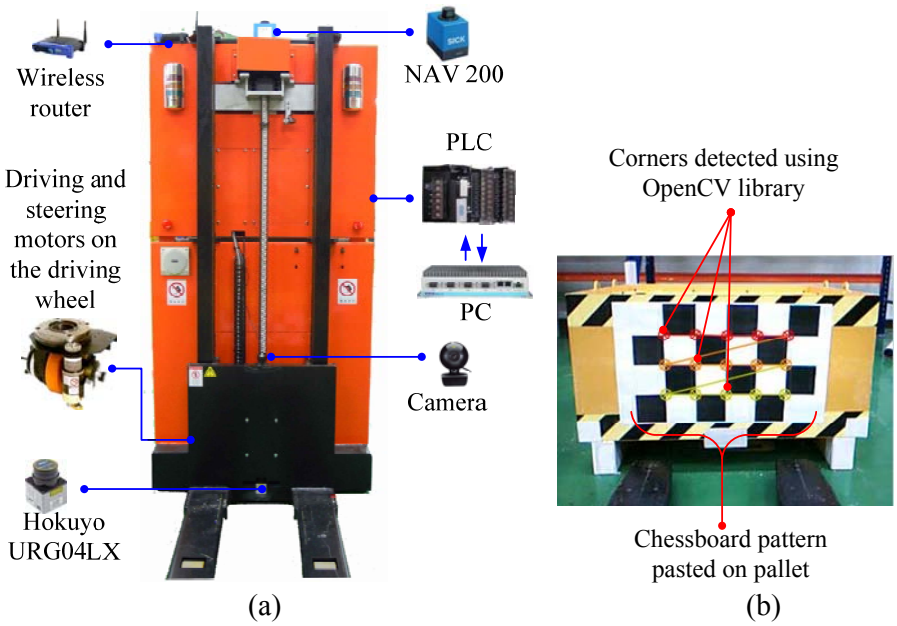

Figure 7. (a) Forklift with sensors and controllers used in experiments. (b) Chessboard pattern pasted on the pallet and its corners as detected by the vision system using the OpenCV library.

From the camera, the position (x, y) and orientation (θ) with respect to the chessboard pattern on the pallet are measured. Then, the variables ρ, α, and ϕ are calculated to implement control laws (18)-(19).

Figure 8 depicts the trajectory of the forklift given by the NAV200 from the initial configuration (−2.32, −1.05, 0.63) to the goal configuration (0, 0, 0). Figures 9-12 show the configuration motions, the orientation error associated with the direction to the goal point (α), the linear velocity, and the steering angle of the vehicle, respectively. The forklift reached (−0.08, 0.013, 0.017) at 35 s. As shown in Figure 10, α remained within the bound of $\bar{\alpha}$ for all time. This indicates that the target image was always inside the camera view. Figures 11 and 12 show the linear velocity and steering angle, respectively.

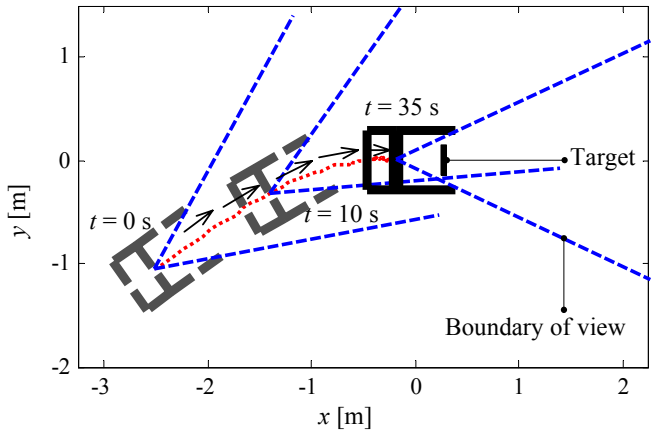

This article can be cited as A. Widyotriatmo and K.-S. Hong, Configuration Control of an Autonomous Vehicle under Nonholonomic and Field-of-View Constraints, International Journal of Imaging and Robotics, vol. 15, no. 3, pp. 126-139, 2015.

Figure 8. Configuration control with FOV constraint (experiment).

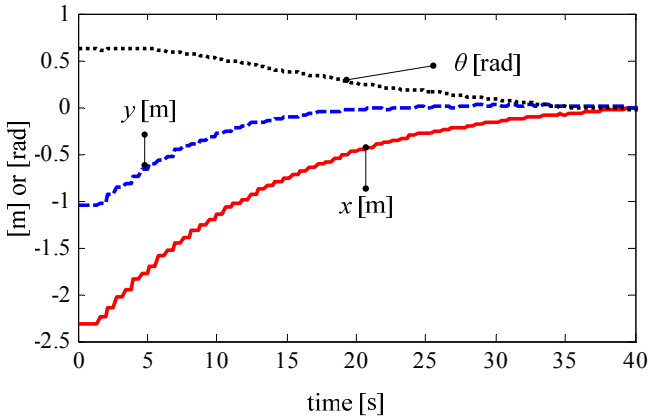

Figure 9. Configuration motions (experiment).

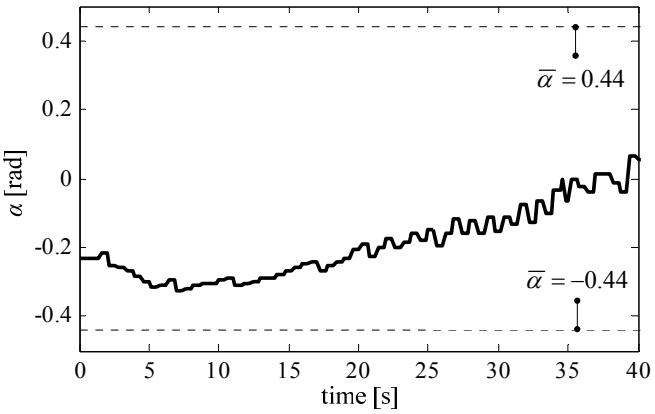

Figure 10. α (experiment).

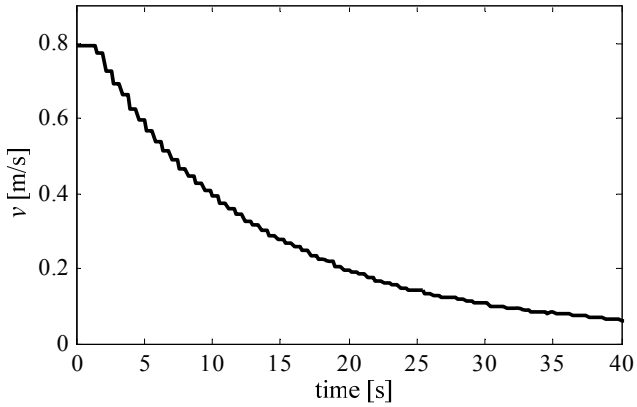

Figure 11. Linear velocity command (experiment).

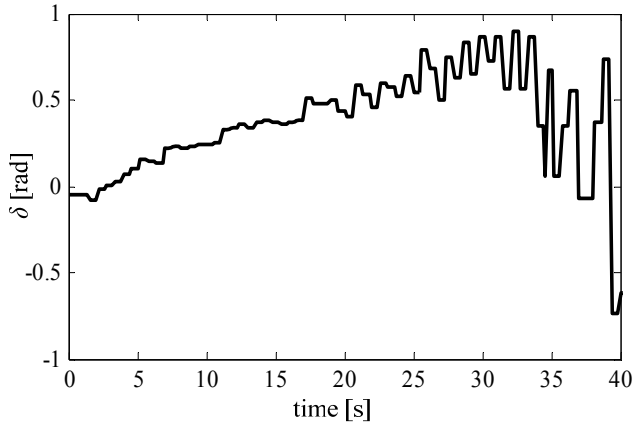

Figure 12. Steering angle command (experiment).

5. CONCLUSIONS

In this paper, an algorithm for controlling a forklift's motion from an initial to a goal configuration using a camera with FOV constraint was developed. The proposed control law derived from a barrier function ensures that the goal feature will be continuously visible through the camera during the vehicle's motion to the goal configuration. The convergence of the vehicle to the goal configuration was guaranteed using the Lyapunov method. The designed gains provide a fast convergence of the states to the origin. Using the control laws with no FOV constraint, the target feature fell outside the FOV of the camera as the vehicle moved. On the other hand, the proposed method maintained the target feature within the camera's FOV while the vehicle moved to the target. The effectiveness of the proposed control law was shown through experimental results of pallet picking of an autonomous forklift.

6. REFERENCES

Amarasinghe, D., Mann, G. K. I., and Gosine, R. G., 2007, Vision-based hybrid control scheme for autonomous parking of a mobile robot. *Advan. Robot.* 21, 905-930.

Becerra, H. M., Lopez-Nicolas, G., Sagues, C., 2011, A sliding-mode-control law for mobile robots based on epipolar visual servoing from three views. *IEEE Trans. Robot.* 27, 175-183.

Bhattacharya, S., Murrieta-Cid, R., Hutchinson, S., 2007, Optimal paths for landmark-based navigation by differential-drive vehicles with field-of-view constraints. *IEEE Trans. Robot*. 23, 47-59.

Gusrialdi, A., Dirza R., Hatanaka, T., Fuita, M., 2013, Improved distributed coverage control for robotic visual sensor network under limited energy storage, *Int. J. Imaging Robot*., 10, S2.

Huusom, J. K., Poulsen, N. K., Jørgensen, S. B., 2010, Iterative feedback tuning of uncertain state space systems, *Brazilian Journal of Chemical Engineering*,. 2, 461-472.

Jafarnejadsani, H., Pieper, J., Ehlers, J., 2013, Adaptive control of a variable-speed variable-pitch wind turbine using radial-basis function neural network, *Control Syst. Technol.*, 21, 2264-2272.

Joelianto, E., Anura, D. C., Priyanto, M. P., 2013, ANFIS – Hybrid Reference Control for Improving Transient Response of Controlled Systems Using PID Controller, *Int. J. Artificial Intelligent*, 10, S13.

Kantor, G., Rizzi, A., 2005, Feedback control of underactuated systems via sequential composition: Visually guided control of a unicycle. In: Dario P., and Chatila, R. (eds.) *Robot. Res.: The Eleventh Int. Symp.,* New York: Springer-Verlag, 15, 281-290.

Lopes, G. A. D., Koditschek, D. E., 2007, Visual servoing for nonholonomically constrained three degree of freedom kinematic systems. *Int. J. Robot. Res*. 26, 715-736.

Lopez-Nicolas, G., Sagues, C., 2011, Vision-based exponential stabilization of mobile robots. *Auton. Robot*. 30, 293-306.

Mariottini, G. L., Oriolo, G., Prattichizzo, D., 2007, Image-based visual servoing for nonholonomic mobile robots using epipolar geometry. *IEEE Trans. Robot*. 23, 87-100.

Ngo, K. B., Mahony, R., Jiang, Z. P., 2005, Integrator backstepping using barrier functions for systems with multiple state constraints. *Proc. 44th IEEE Conf. Decision and Control,* Seville, Spain, 8306–8312.

Pásztó, P., Kľúčik,M., Chovan, L., Tölgyessy, M., Hanzel, J., Quang, K. D., Hubinský, P., 2014, Object relative position estimation based on Hough transform using one camera, *Int. J. Imaging Robot*., 13, 2.

Precup, R.-E., Preitl, St., Rădac, M.-B., Petriu, E. M., Dragoş, C.-A. and Tar, J. K., 2010, Experiment-based teaching in advanced control engineering. *IEEE Trans. Education*, 54, 345-355.

Salaris, P., Fontanelli, D., Pallatino, L., 2010, Shortest paths for a robot with nonholonomic and field-of-view constraints*. IEEE Trans. Robot.* 26, 269-281.

Seelinger, M., Yoder, J.-D., 2006, Automatic visual guidance of a forklift engaging a pallet. *Robot. Auton. Syst*. 54, 1026-1038.

Siegwart, R., and Nourbakhsh, I. R., 2004, *Introduction to Autonomous Mobile Robots*, MA: MIT Press.

Tamba, T. A., Hong, B., Hong, K.-S., 2009, A path following control of an unmanned autonomous forklift. *Int. J. Control. Autom.* 7, 113-122.

Tee, K. P., Ge, S. S., Tay, E. H., 2009, Barrier Lyapunov functions for the control of output-constrained nonlinear systems. *Automatica* 45, 918-927.

Van Den Berg, J., Abbeel, P., Goldberg, K., 2011, LQG-MP: Optimized path planning for robots with motion uncertainty and imperfect state information. *Int. J. Robot. Res.* 30, 895-913.

Widyotriatmo, A., Hong, B., Hong, K.-S., 2009, Predictive navigation of an autonomous vehicle with nonholonomic and minimum turning radius constraints. *J. Mech. Sci. Technol.* 23, 381-388.

Widyotriatmo, A., Hong, K.-S., Prayudhi, L. H., 2010, Robust stabilization of a wheeled vehicle: Hybrid feedback control design and experimental validation. *J. Mech. Sci. Technol.* 24, 513-520.

Widyotriatmo, A., Hong, K.-S., 2011, A navigation function-based control of multiple wheeled vehicles. *IEEE Trans. Indust. Electron.* 57, 1896-1906.

Widyotriatmo, A., Hong, K.-S., 2012, Switching algorithm for robust configuration control of a wheeled vehicle, *Control Eng. Pract.* 20, 315-325.

Widyotriatmo, A., Pamosoaji, A. K., Hong, K.-S., 2013, Control architecture of an autonomous material handling vehicle, *Int. J. Artif. Intell.* 8, S12.

Zhang, H., Ostrowski, J. P., 2002, Visual motion planning for mobile robots. *IEEE Trans. Robot. Automat.* 18, 199-208.